Chemical Engineering Journal 154 (2009) 348–354

Contents lists available at ScienceDirect

Chemical Engineering Journal

journal homepage: www.elsevier.com/locate/cej

Towards practical application of lanthanum ferrite catalysts for NO reduction with H_2

Stefania Furfori, Samir Bensaid, Nunzio Russo, Debora Fino*

Department of Materials Science and Chemical Engineering, Politecnico di Torino, Corso Duca degli Abruzzi 24, 10129 Torino, Italy

ARTICLE INFO

Article history:
Received 16 December 2008
Received in revised form 4 March 2009
Accepted 5 March 2009

Keywords:
Selective catalytic reduction of NO
Perovskite
Palladium
Hydrogen

ABSTRACT

A series of perovskite-type catalysts ($LaFeO_3$, $La_{0.8}Sr_{0.2}FeO_3$, $Pd/La_{0.8}Sr_{0.2}FeO_3$, $La_{0.8}Sr_{0.2}Fe_{0.9}Pd_{0.1}O_3$, $La_{0.7}Sr_{0.2}Ce_{0.1}FeO_3$, $Pd/La_{0.7}Sr_{0.2}Ce_{0.1}FeO_3$ and $La_{0.7}Sr_{0.2}Ce_{0.1}Fe_{0.9}Pd_{0.1}O_3$) has been prepared by the solution combustion synthesis method and fully characterized by XRD, BET, FESEM and TPD/R analyses. The performance of these catalysts towards the NO reduction mechanism by H_2 has been evaluated in a temperature-programmed reaction apparatus (TPRe) in the absence and in the presence of oxygen. The catalysts have been studied in the 25–350 °C temperature range, and significant catalytic activities were measured at 150–250 °C. Among the catalysts screened, $La_{0.8}Sr_{0.2}Fe_{0.9}Pd_{0.1}O_3$, showed the best performance. Hence, it was deposited directly over a ceramic honeycomb monolith by *in situ* SCS, tested in a lab-scale test rig, then submitted to the specific ageing protocol (thermal treatment at 500 °C for 96 h) in the presence of water vapour and sulfur dioxide, two potentially deactivating species present in diesel exhaust gases, and it showed a good compromise between satisfactory catalytic activity and stability. A mechanistic analysis is presented concerning the relationship between the observed activity and the reducibility of the B site, determined through TPR experiments. Some final conclusions are drawn on the perspective of the practical application of the investigated aftertreatment route for diesel exhaust gases.

1. Introduction

Road transport is one of the main contributors to hydrocarbon (HC), nitrogen oxides (NO_x) and particulate matter (PM) emissions in the atmosphere. The prevalent technology available to control NO_x emission is the selective catalytic reduction (SCR) by NH_3, a technology that is based above all on V catalysts, which dominate the market of stationary applications but are also being considered in exhaust gas treatments for heavy duty vehicles [1]. The weak points of this technology in mobile applications are: (i) NH_3 storage, which forces the use of complex urea storage and hydrolysis systems [2]; (ii) the release of V into the environment, which is now leading to the development of specific V-free catalysts [3–6]. As an alternative option, the use of CO and light hydrocarbons, whether already present in the vehicle exhaust or introduced/generated on purpose, has been extensively studied in the search for alternative reducing agents [7–10]. Perovskite-like mixed oxides in particular have been extensively investigated for NO_x reduction by CO [11–16]. More recently, a number of research groups have explored the use of hydrogen as a reductant and the results are promising [17–25]. Hence, within the framework of a European research project [26], the authors started an investigation with leading industrial companies, on the adoption of a small on board reformer for H_2 generation from diesel oil for direct injection into the exhaust line ahead of the aftertreatment catalysts to promote NO_x SCR by H_2 in diesel exhaust treatment.

The work here presented concerns the synthesis, characterization, catalytic activity tests and the reaction mechanism assessment of a series of lanthanum ferrite perovskites, whose performances towards NO reduction have been evaluated both in the presence and in the absence of oxygen, in an attempt to find a correlation between catalyst structure and activity. Some conclusions have been drawn concerning the role of the B site element on the activity of the catalyst and a possible reaction mechanism. The performance of the most promising developed catalyst, once deposited on a honeycomb catalytic converter and tested in a lab-scale test rig, has also been presented and discussed. Moreover, the stability of the most interesting catalyst produced, deposited on a cordierite monolith, aged at different operating temperatures and gaseous atmospheres has also been assessed. Finally, on the basis of the obtained results, the suitability of the mentioned catalysts for the treatment of the diesel engine exhausts has been discussed.

2. Experimental

2.1. Catalyst preparation

A series of perovskite catalysts ($LaFeO_3$, $La_{0.8}Sr_{0.2}FeO_3$, $La_{0.8}Sr_{0.2}Fe_{0.9}Pd_{0.1}O_3$, $La_{0.7}Sr_{0.2}Ce_{0.1}FeO_3$ and $La_{0.7}Sr_{0.2}Ce_{0.1}Fe_{0.9}$

* Corresponding author. Tel.: +39 011 090 4710; fax: +39 011 090 4699.
E-mail address: debora.fino@polito.it (D. Fino).

1385-8947/$ – see front matter © 2009 Elsevier B.V. All rights reserved.
doi:10.1016/j.cej.2009.03.009

$Pd_{0.1}O_3$) were prepared by solution combustion synthesis (SCS) from aqueous solutions of metal nitrates (acting as oxidizers) and urea (acting as an internal sacrificial fuel). According to this method, the reagents (Fluka extra pure grade) are first dissolved in distilled water in stoichiometric amounts. The obtained solution is then placed in an oven and kept at a constant temperature (650 °C) in calm air. Under such conditions, boiling is quickly induced and the solution froths and swells until the synthesis reactions start. Combustion is over in a few seconds. Under these conditions, nucleation of metal oxide crystals is induced, their growth is limited and nano-sized crystals are obtained [27].

To strengthen its practical application potential, this method, suitably adapted according to an *in situ* version, was also demonstrated to be amenable for the deposition of mixed oxides of catalysts within a honeycomb catalytic converter [28].

Finally, in a couple of other preparations ($Pd/La_{0.8}Sr_{0.2}FeO_3$ and $Pd/La_{0.7}Sr_{0.2}Ce_{0.1}FeO_3$), Pd was not included in the reaction mixture of the precursors but deposited over pre-formed perovskites via incipient wetness impregnation IWI with an aqueous solution of Pd nitrate. The prepared powders are dried in an oven at 120 °C for 12 h, then calcined in air at 500 °C for 5 h in order to decompose the nitrate and obtain small and well dispersed palladium clusters over the perovskite surface.

It should be underlined that all the elements included in the catalyst formulations are compatible with the devised application, as they are widely employed in three-way catalysts (Pd, Ce and La) and not harmful (Fe). This is not a trivial condition and it significantly limits the possible perovskite compositions.

2.2. Catalyst characterization

X-ray diffraction (PW1710 Philips diffractometer equipped with a monochromator, Cu Kα radiation) was used to check the achievement of the perovskites oxide structure and to assess their purity, crystalline structure and approximate crystal grain size.

A field emission scanning electron microscope (FESEM—Leo 50/50 VP with GEMINI column) was employed to analyze the microstructure of the crystal catalyst aggregates and to assess the size and the morphology of the oxide crystals themselves.

The BET-specific surface area of the catalysts has been evaluated from the linear parts of the BET plots of the N_2 isotherms, using a Micromeritics ASAP 2010 analyzer.

Some temperature-programmed analyses were performed in a Thermoquest TPD/R/O 1100 analyzer, equipped with a thermal conductibility detector (TCD). A fixed catalyst bed (100 mg) was enclosed in a quartz tube and sandwiched between two quartz wool layers; prior to each temperature-programmed oxygen desorption (TPD) run, the catalyst was heated under an O_2 flow (40 N ml/min) up to 750 °C. After 30 min at this temperature, as a common pre-treatment, the temperature was lowered to 25 °C under the same oxygen flow rate, thereby achieving complete saturation. Afterwards, He was fed to the reactor at a 10 ml/min flow rate and kept for 1 h at room temperature in order to purge any excess of oxygen. The catalyst was then heated to 950 °C at a constant heating rate of 10 °C/min under the same helium flow. The total amount of O_2 desorbed during the heating protocol was detected by the TCD detector after proper calibration.

Temperature-programmed reduction (TPR) experiments were also carried out in the same apparatus. After the same oxidation pre-treatment adopted for the TPD runs, the sample was reduced with a 4.95% H_2/Ar mixture (10 N ml/min) meanwhile heating it at a 10 °C/min rate up to 950 °C. Once again, the amount of converted H_2 was monitored via the TCD detector.

2.3. Catalytic activity tests

The activity of the prepared catalysts was analyzed through temperature-programmed reaction (TPRe), according to a standard operating procedure: a gas mixture (1000 ppmv NO, 4000 ppmv H_2, He balance) was fed at the constant rate of 300 Nml/min via a set of mass flow controllers to the catalytic fixed-bed microreactor which was kept in an electric oven. The tubular quartz reactor was loaded with 100 mg of catalyst powder and 500 mg of silica pellets (0.3–0.7 mm in size); this inert material was added to reduce the specific pressure drop across the reactor. The W/F of the gases through the catalytic bed was about 0.02 g/(s cm^3) (equivalent to a GHSV of 30,000 h^{-1} on a real car aftertreatment converter). The reaction temperature was varied in the PID-regulated oven from room temperature to 350 °C in fixed steps (every 10–20 °C). The outlet gas composition was monitored at each temperature step using a $CO/CO_2/N_2O$ NDIR (ABB) and NO/NO_2 chemiluminescence analyzer (Eco Physics) as well as by a quadrupole detector (Baltzer Quadstar 422). The temperature corresponding to half NO conversion (T_{50}) was taken as an activity index of each tested catalyst.

The performance of the most promising catalyst, $La_{0.8}Sr_{0.2}Fe_{0.9}Pd_{0.1}O_3$, was analyzed in the presence of 5% oxygen (1000 ppmv NO, 10000 ppmv H_2, 5 vol.% O_2, He balance; W/F = 0.02 g/(s cm^3)) at three different space velocities (20,000–30,000–40,000 h^{-1}) to check the influence of this operating parameter and derive some provisional indications on the reaction mechanism.

2.4. Catalyst monolith preparation, characterization and activity assessment

The $La_{0.8}Sr_{0.2}Fe_{0.9}Pd_{0.1}O_3$ was then deposited on a honeycomb support (cylindrical cordierite honeycomb; diameter: 35 mm; length: 25 mm; cell density: 200 cpsi; manufacturer: CTI) via the following steps:

- a preliminary deposition of a layer of γ-alumina (5 wt% referring to the monolith weight) by *in situ* SCS [27];
- subsequent deposition of 20 wt% (referring to the monolith weight) of the most active developed catalyst, once again by *in situ* SCS.

A calcinations step was finally performed at 700 °C for 2 h in air on all the catalytic monoliths prepared as a common post-treatment.

Adhesion tests and structural characterization (XRD and FESEM) were carried out. The adhesion properties between the catalyst and ceramic surface were checked by means of an ultrasonic bath test: a piece of the catalytic monolith was weighed before and after the ultrasonic treatment to quantify the catalyst loss.

Physicochemical characterization was performed on sections of the catalytic monolith; in particular, FESEM-EDS analyses were performed using the previously reported apparatus, in order to investigate the morphology and composition of the deposited catalytic layer.

The catalytic NO reduction experiments were performed in a stainless steel reactor, heated in a horizontal split tube furnace, with a heating length of 60 cm. The catalyzed monolith was sandwiched between two mullite foam discs to optimize flow distribution. A thermocouple, inserted along one of the central monolith channels, was used to measure the inlet monolith temperature. Standard feed conditions (100 ppmv NO, 1000–2000–4000 ppmv H_2, with and without 5% O_2, N_2 balance) were ensured through the use of mass flow controllers. The upstream and downstream reactor temperature difference, measured in the axial direction, was not very significant (<20 °C). The gas hourly space velocity (GHSV) was

set equal to 30,000 h^{-1}, whereas the composition of the outlet gas stream was monitored by the previously described analytical equipment used for the TPRe tests.

2.5. Catalytic monolith ageing procedure

A catalyst used for NO_x reduction in diesel emissions may loose its effectiveness for several reasons: temporary temperature rises, a poisoning effect caused by some diesel exhaust components (e.g. SO_2, H_2O), prolonged working time at high temperatures. In order to consider the effect of each of these factors separately, ageing treatments were performed on a catalytic monolith under the following conditions:

- thermal ageing in N_2 at 500 °C for 96 h containing 12 vol.% of moisture obtained from humidification in a thermostasized bubble column;
- thermal ageing, at the same temperatures, in N_2 containing 50 ppmv SO_2, a larger value than current SO_2 levels in exhaust gases (a few ppms).

All these treatments were carried out in a tubular furnace with a gaseous flow of 100 ml/min. In addition, the possible loss of catalytic activity due to prolonged catalyst operation was checked. This treatment was repeated using the same catalyst monolith in order to carry out up to six consecutive reduction cycles. Most of the physical and chemical characterization analyses described above were replicated on aged catalytic monoliths.

The tests on the monoliths, after the ageing treatment, were carried out under the same operating conditions as the experiments on fresh monoliths using the same apparatus and analysis systems reported above.

3. Results and discussion

Fig. 1 illustrates the XRD spectra recorded for all the catalysts synthesized in the present study: it shows diffraction peaks that correspond to the desired catalyst structures and confirms the presence of a crystalline lanthanum ferrite phase which is substantially preserved after all of the La or Fe substitutions imposed. However, since the detection limit of this technique is 4 wt%, the presence of amorphous or minor crystalline phases cannot be completely excluded.

Fig. 2 shows a FESEM picture of the $La_{0.8}Sr_{0.2}FeO_3$ perovskite catalyst produced via SCS. However, it is representative of all the prepared catalysts. The FESEM view of the microstructure of the crystal aggregates of the $La_{0.8}Sr_{0.2}FeO_3$ catalyst highlights the very foamy structure, which is typical of all catalysts synthesized by SCS.

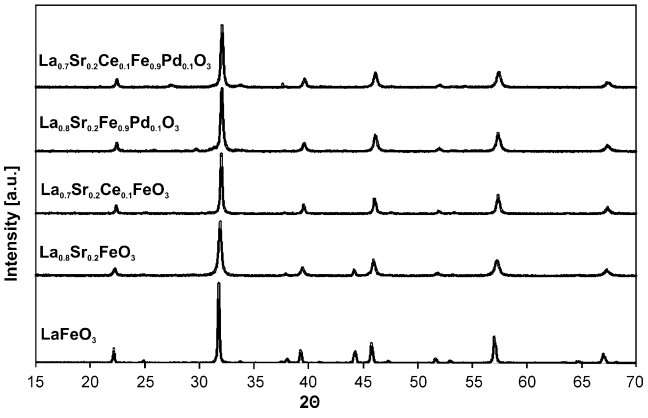

Fig. 1. XRD diffraction patterns of all the catalysts synthesized.

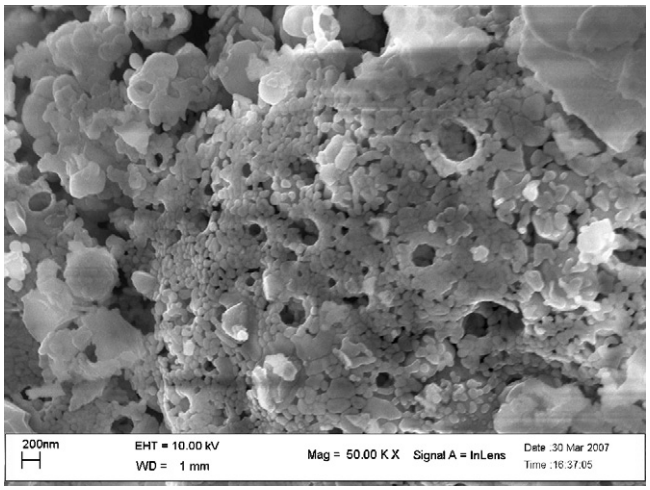

Fig. 2. FESEM micrograph of the $La_{0.8}Sr_{0.2}FeO_3$ catalyst crystals.

The BET specific surface area (SSA) values range from between 3 and 19 m^2/g, as listed in Table 1, where the temperature corresponding to half the NO conversion (T_{50}) and the amount of H_2 consumed during the TPR analysis are also reported for all of the investigated catalysts.

As expected, all the catalysts significantly lower the NO reduction peak temperature compared with that of the non-catalytic reduction and with that of the standard $LaFeO_3$. By comparing the activity results for all the investigated catalysts (Table 1) under the same operating conditions (1000 ppmv NO; 4000 ppmv H_2; He = balance), an activity order can be outlined as follows:

- the $La_{0.9}Sr_{0.2}Fe_{0.9}Pd_{0.1}O_3$ shows the best activity (T_{50} = 130 °C);
- the other substituted perovskite catalysts exhibit quite similar activities (T_{50} = 210–280 °C);
- the unsubstituted $LaFeO_3$ is the least active catalyst (T_{50} = 350 °C);
- all the perovskites exhibit a catalytic effect compared to the reference silica pellets, an effect which entail T_{50} values of 595 °C.

Fig. 3 compares the catalytic reduction of NO to N_2 in the absence and in the presence of 5% oxygen for the best tested catalysts ($La_{0.8}Sr_{0.2}Fe_{0.9}Pd_{0.1}O_3$) as a function of the equivalent GHSV. The complete NO conversion to N_2 on $La_{0.8}Sr_{0.2}Fe_{0.9}Pd_{0.1}O_3$ is achieved at 150–200 °C. Complete conversion is never reached in the presence of oxygen, and the maximum conversion is about 75% at 160 °C. When the oxygen is present in the feed stream, other NO_x products (N_2O, NO_2) are, however, detected. Based on the data plotted in Fig. 4, a part of the conversion of NO to N_2 can be attributed to kinetic limitations at low temperatures and to the formation of N_2O and NO_2 at high temperatures. Good selectivity to N_2 formation is only

Table 1
Collection of catalyst characterization results concerning the BET specific surface area, catalytic activity (half NO conversion temperature) and the temperature-programmed reduction with H_2.

Catalyst	BET (m^2/g)	T_{50} (°C)	H_2 consumed in TPR runs (μmol/g)
$LaFeO_3$	8.9	350	38.62
$La_{0.8}Sr_{0.2}FeO_3$	11.7	220	270.93
$La_{0.8}Sr_{0.2}Fe_{0.9}Pd_{0.1}O_3$	7.1	130	380.22
$Pd/La_{0.8}Sr_{0.2}FeO_3$	11.4	210	283.31
$La_{0.7}Sr_{0.2}Ce_{0.1}FeO_3$	3.7	280	271.69
$La_{0.7}Sr_{0.2}Ce_{0.1}Fe_{0.9}Pd_{0.1}O_3$	6.6	215	139.98
$Pd/La_{0.7}Sr_{0.2}Ce_{0.1}FeO_3$	18.8	225	153.83
Non-catalytic reaction	–	595	–

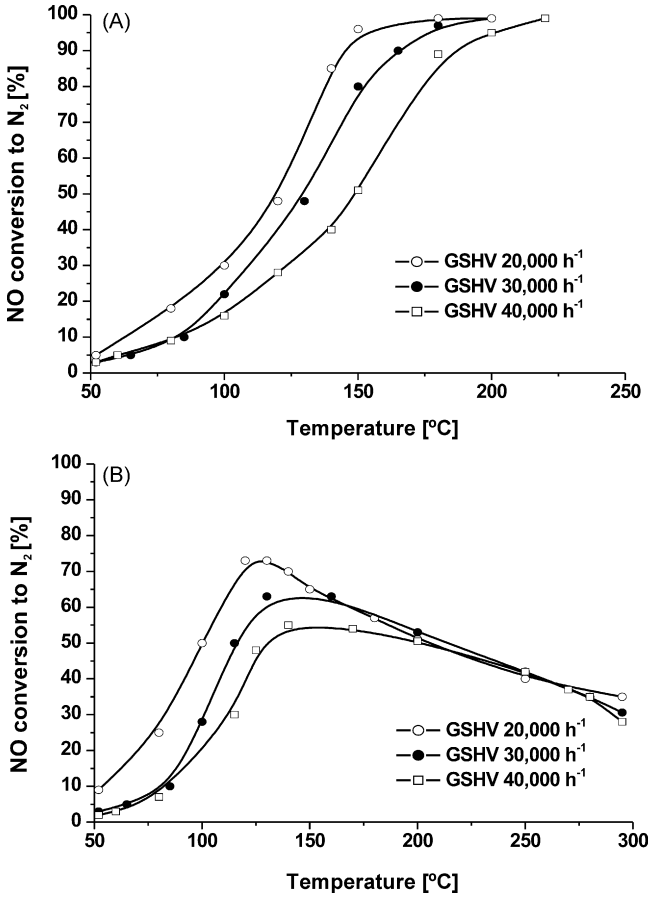

Fig. 3. NO conversion to N_2 on powder $La_{0.8}Sr_{0.2}Fe_{0.9}Pd_{0.1}O_3$: (A) 1000 ppmv NO, 4000 ppmv H_2, He balance; (B) 1000 ppmv NO, 10000 ppmv H_2, 5% O_2, He balance.

achievable at low temperatures (i.e. <125 °C) for the experimental conditions tested. Some further investigations to devise tentative reaction mechanisms were therefore undertaken, as a first step in the attempt to design a more effective catalyst.

Fig. 5 shows the results obtained during the hydrogen TPR runs. By comparing the activity order of the synthesized catalysts with the TPR curves, a correlation can be confirmed between the level of B site reduction and the activity of the perovskite for NO_x reduction.

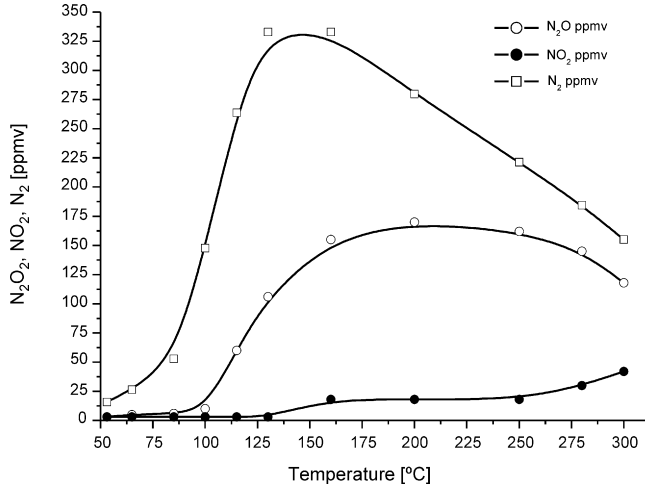

Fig. 4. NO conversion to N_2O, NO_2, N_2 on powder $La_{0.8}Sr_{0.2}Fe_{0.9}Pd_{0.1}O_3$: 1000 ppmv NO, 10000 ppmv H_2, 5% O_2, He balance, GSHV = 30,000 h^{-1}.

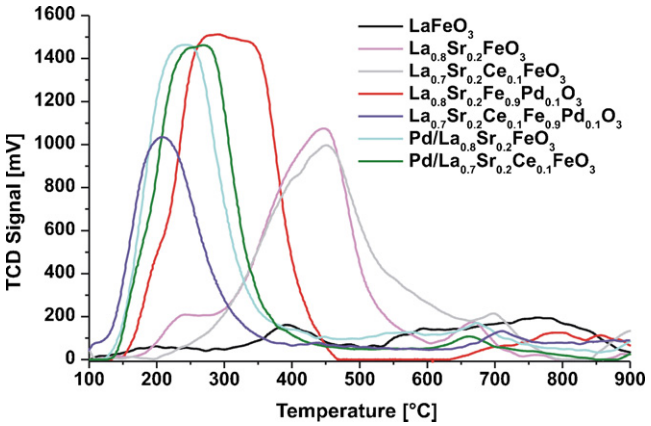

Fig. 5. Results of the TPR tests on all the investigated perovskite catalysts.

The most active catalyst, $La_{0.8}Sr_{0.2}Fe_{0.9}Pd_{0.1}O_3$, shows the highest amount of H_2 consumed during the TPR analysis.

Fig. 6, which reports the results of the TPD runs, shows that none the perovskite samples have a tendency to release oxygen spontaneously at the temperatures of interest for the studied reaction. Only the most active catalyst, $La_{0.8}Sr_{0.2}Fe_{0.9}Pd_{0.1}O_3$, shows some perceivable oxygen release above 800 °C.

Both the TPR and TPD analyses indicate that the $La_{0.8}Sr_{0.2}Fe_{0.9}Pd_{0.1}O_3$ compound is the most prone to redox cycles among those studied.

Voorhoeve et al. [29] were among the first to address the mechanism of NO reduction with H_2 in the absence of oxygen over perovskite catalysts. These authors concluded that the reaction mechanism involves the reduction of the catalyst, followed by NO adsorption. The high catalytic activity of perovskite catalysts is quite often related to their defective structure [18,20]. Oxygen vacancies may offer suitable sites for NO adsorption and dissociation [20]. The formation of oxygen vacancies may be favoured by the partial substitution of the A and B sites of the $LaFeO_3$ catalyst with other cations.

As proven by TPR experiments, the partial substitution of the A site cation, La^{3+}, with another cation of different oxidation states, Sr^{2+} and Ce^{4+}, enhances the ability of the catalyst to reduce compared to the basic $LaFeO_3$ catalyst and the formation of anion or cation vacancies, respectively, occurs when Sr^{2+} or Ce^{4+} metal cations are introduced. The deposition of Pd onto the catalyst with substituted A sites ($La_{0.8}Sr_{0.2}FeO_3$ and $La_{0.7}Sr_{0.2}Ce_{0.1}FeO_3$) causes a further increase in the ability of the catalyst to reduce, i.e. the temperature at which reduction starts is lowered. As reported in the

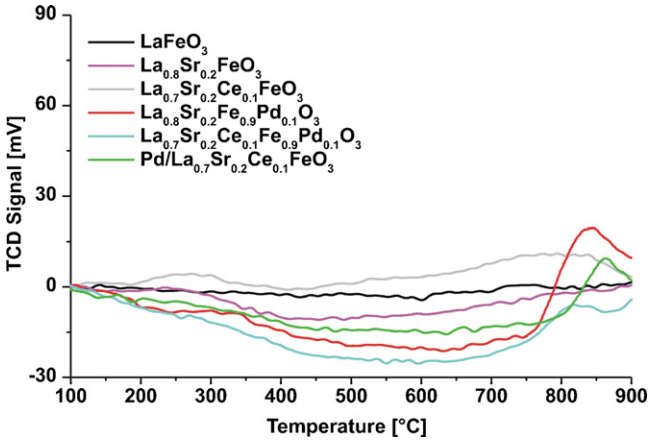

Fig. 6. Results of the oxygen TPD tests on all the investigated perovskite catalysts.

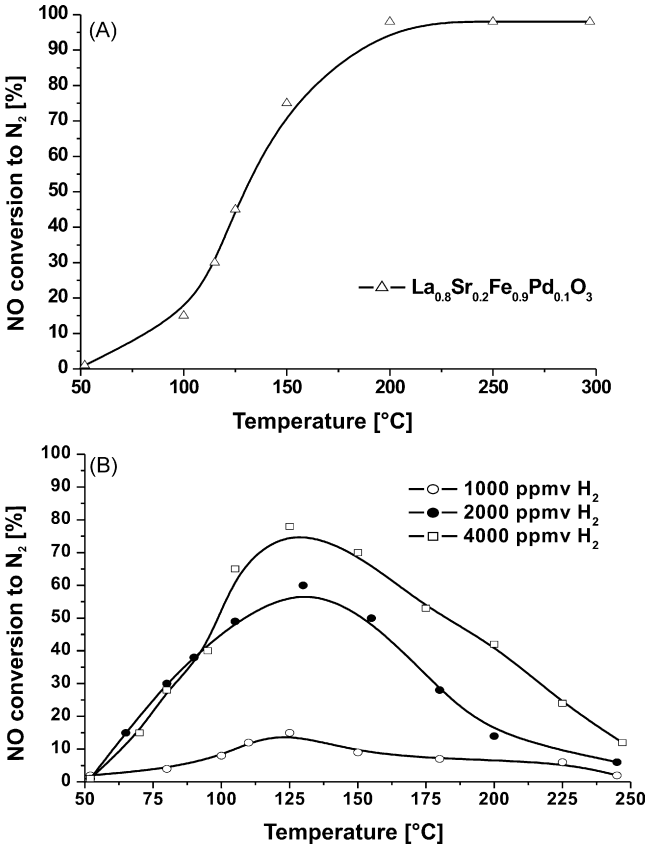

Fig. 7. NO conversion to N_2 in NO + H_2 reaction over $La_{0.8}Sr_{0.2}Fe_{0.9}Pd_{0.1}O_3$ deposited on a honeycomb cordierite monolith; GSHV = 30,000 h^{-1}: (A) 100 ppmv NO, 1000 ppmv H_2, N_2 balance; (B) 100 ppmv NO, 1000–2000–4000 ppmv H_2, 5% O_2, N_2 balance.

literature in [24,25], the involvement of active sites where Pd and anionic vacancies cooperate in the NO/H_2 reaction is possible. This is likely due to the H_2 chemisorption function of palladium which may provide the perovskite grains close to the Pd clusters (a few nanometers large, as measured by HRTEM) with active hydrogen species.

The best performance was found when the B site was partially substituted with Pd and the A site with strontium, as shown by the wider H_2 reduction peak areas in the TPR curves. The insertion of palladium onto the B site should promote a change in the Fe^{4+} oxidation state and possibly favour more intensive redox opportunities for NO and H_2 chemisorption.

According to the work by Ferri et al. [20], the NO reduction mechanism of H_2 over oxide catalysts involves a process that involves several reactions.

$$NO_{ad} + * \rightarrow NO_{ad} \quad (1)$$

$$NO_{ad} + NO \rightarrow N_2O + O_{ad} \quad (2)$$

$$2NO_{ad} \rightarrow 2N_{ad} + O_2 \quad (3)$$

$$NO_{ad} + N_{ad} \rightarrow N_2O + * \quad (4)$$

$$2NO_{ad} \rightarrow N_2 + 2O_{ad} \quad (5)$$

$$2O_{ad} \rightarrow O_2 + 2* \quad (6)$$

According to this scenario, reactions (1) and (5) should govern the NO process reduction to N_2 at low temperatures, whereas at higher temperatures, the formation of N_2O as an intermediate could be attributed to reactions (2)–(4). The experimental data seem to suggest that only above certain temperatures does the Eley–Rideal mechanism of reaction (2) produce significant effects.

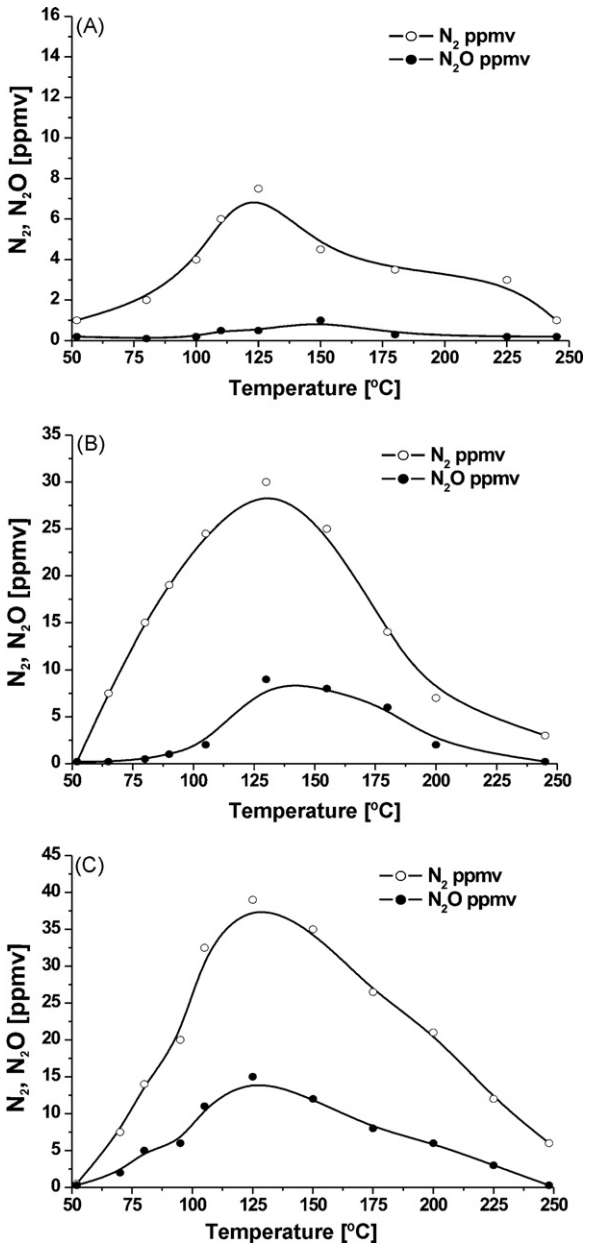

Fig. 8. NO conversion to N_2O, N_2 in NO + H_2 reaction over $La_{0.8}Sr_{0.2}Fe_{0.9}Pd_{0.1}O_3$ deposited on a honeycomb cordierite monolith; GSHV = 30,000 h^{-1}: (A) 100 ppmv NO, 1000 ppmv H_2, 5% O_2, N_2 balance; (B) 100 ppmv NO, 2000 ppmv H_2, 5% O_2, N_2 balance; (C) 100 ppmv NO, 4000 ppmv H_2, 5% O_2, N_2 balance.

According to the above mechanistic scenario, it is quite clear that the presence of oxygen plays a negative role. Oxygen reduces the oxygen vacancies and the Pd active sites through direct chemisorption, as previously explained in [30]. Furthermore, as shown in Fig. 4, it actually promotes NO-to-NO_2 oxidation, which is only limited by the related thermodynamic constraints [31].

Deeper investigations, e.g. by FTIR spectroscopy, might be useful to provide further evidence on the above reaction pathways and possibly suggest the design of new catalysts. However, since this paper has the aim of providing a provisional assessment of the application potential of this technology, some experiments were undertaken on a catalyst-lined honeycomb converter similar to those currently employed in car exhaust gas aftertreatment systems.

The most active catalyst, $La_{0.8}Sr_{0.2}Fe_{0.9}Pd_{0.1}O_3$, was deposited on a cordierite substrate, coated with γ-alumina. The promising

Table 2
TPRe half conversion and peak temperatures and the maximum conversion rate after the ageing treatments at different operating conditions over $La_{0.8}Sr_{0.2}Fe_{0.9}Pd_{0.1}O_3$ deposited on a honeycomb cordierite monolith.

Feed conditions	Ageing procedure	T_{50} (°C)	T_p (°C)	η_p (%)
No O_2 NO:H_2 1:10	Fresh	130	200	99.0
	Aged 500 °C 12% H_2Ov	131	204	96.0
	Aged 500 °C 50 ppmv SO_2	129	202	96.5
	6th reduction cycles	135	206	99.0
5% O_2 NO:H_2 1:10	Fresh	100	125	15.0
	Aged 500 °C 12% H_2Ov	90	128	7.8
	Aged 500 °C 50 ppmv SO_2	95	126	8.0
5% O_2 NO:H_2 1:20	Fresh	110	130	58.0
	Aged 500 °C 12% H_2Ov	93	132	45.5
	Aged 500 °C 50 ppmv SO_2	96	130	45.0
5% O_2 NO:H_2 1:40	Fresh	105	128	78.0
	Aged 500 °C 12% H_2Ov	99	126	69.0
	Aged 500 °C 50 ppmv SO_2	100	125	69.5

performance of this catalyst was also confirmed in the structured form when supported on the monolith: without oxygen at GSHV = 30,000 h^{-1}, T_{50} was equal to 130 °C (see Fig. 7A) with a complete NO reduction at about 200 °C. However, in the presence of oxygen (5 vol%), at least a two-fold higher hydrogen concentration (NO:H_2 molar ratio from 1:10 to 1:20) was required to achieve approximately the same NO to N_2 reduction level obtained with the catalyst in the powder form (see Fig. 7B). In view of a practical applications perspective, further improvement of this performance is expected. The presence of diesel exhaust gases is a *conditio sine qua non* and the availability of a specifically generated H_2 rich stream entails fuel penalties that could become unacceptable. It was evaluated that a 4% fuel penalty is needed to achieve a 2000 ppmv hydrogen concentration ahead of the catalytic converter via a tailored auto-thermal reformer. In order to have a good basis for comparison, the reader should consider that modern diesel particulate trap regeneration routes (based on fuel post-injection and subsequent catalytic combustion to increase the trap temperature to a soot ignition level of 550 °C) entail a fuel penalty of about only 2%.

As a positive feature of the performance of the structured catalyst vs. the powder one, Fig. 8 shows that the relative ratio of the reduced N_2 and N_2O products is more favourable for the structured catalyst. Moreover, if the H_2 concentration in the feed plays a favourable role on NO conversion, as expected, it would also seem to boost N_2O formation slightly more than N_2 formation, in particular for the aged samples, as previously observed in [21]. This is another reason apart from the unacceptable increase in fuel penalties, to try and develop catalysts with higher and higher activity thereby reduce the amount of hydrogen required in the feed.

Finally, a prerequisite for practical applicability of a catalyst is not only its activity but also its stability. Table 2 shows that no serious deactivation was found after the very severe ageing test. An increase of a few centigrade degrees was noticed after the ageing treatment. Further runs were then performed in order to check whether the catalyst remains stable after repeated reduction cycles. The obtained T_{50} data confirm that the activity remains almost unaffected.

4. Conclusions

Several perovskite-type oxide catalysts ($LaFeO_3$, $La_{0.8}Sr_{0.2}FeO_3$, $Pd/La_{0.8}Sr_{0.2}FeO_3$, $La_{0.8}Sr_{0.2}Fe_{0.9}Pd_{0.1}O_3$, $La_{0.7}Sr_{0.2}Ce_{0.1}FeO_3$, $Pd/La_{0.7}Sr_{0.2}Ce_{0.1}FeO_3$ and $La_{0.7}Sr_{0.2}Ce_{0.1}Fe_{0.9}Pd_{0.1}O_3$) were developed for the selective catalytic reduction of NO to N_2 and H_2O by hydrogen, both in the presence and absence of oxygen. The solution combustion synthesis technique was adopted successfully to produce in an easy, low-cost and quick one-step process catalyst with a rather high surface area and purity. The same technique, adapted for *in situ* catalyst generation, was used to deposit the catalyst on ceramic structured supports with a very high surface area. The presented results have demonstrated that the catalytic activity of the prepared perovskite oxides essentially depends on the B site reduction and on the presence of oxygen vacancies that are suitable for NO adsorption. The $La_{0.8}Sr_{0.2}Fe_{0.9}Pd_{0.1}O_3$ perovskite-type oxide exhibited the highest activity as a consequence of its greater capability to reduce at comparatively low temperatures during the TPR runs, a key requirement for selective catalytic reduction of NO_x by hydrogen.

The results obtained at a converter stage are promising though not completely satisfactory in view of a direct application. On the one hand, the maximum achieved conversion of NO into N_2 is encouraging (60–70%) for GHSV of practical interest and the temperature of optimal performance is quite compatible with the end of the exhaust line of a diesel passenger car. This would correspond to a rather unusual location of the catalyst brick which, however, would lead to no serious drawbacks. On the other hand, the fuel penalty entailed by the technique is still too high (at least 4%).

The ageing of the most promising catalyst, $La_{0.8}Sr_{0.2}Fe_{0.9}Pd_{0.1}O_3$, lined on a honeycomb converter, shows that the thermal ageing did not modify the catalytic monolith stability. No serious deactivation was found: the T_{50} increase noticed after the ageing treatment and consecutive reduction cycles was within 7–10 °C and the maximum conversion rate, in the presence of oxygen, was decreased by 10–15%.

Studies are now in progress in various directions:

- To improve the catalyst selectivity in the presence of oxygen, by maximizing N_2 and lowering N_2O and NO_2 production.
- To understand and possibly close the performance gap between catalysts in powder form and lined over honeycomb monoliths.
- To perform an analysis with a suitable system model, in order to highlight any possible reformer-aftertreatment line strategies that could minimize fuel penalties for a given catalyst performance.

References

[1] P. Forzatti, Present status and perspectives in de-NO_x SCR catalysis, Appl. Catal. A 222 (2001) 221–236.
[2] U.G. Alkemade, B. Schumann, Engines and exhaust after treatment systems for future automotive applications, Solid State Ionics 177 (2006) 2291–2296.
[3] Q. Gongshin, R.T. Yang, Performance and kinetics study for low-temperature SCR of NO with NH_3 over MnO_x–CeO_2 catalyst, J. Catal. 217 (2003) 434–441.
[4] J. Huang, Z. Tong, Y. Huang, J. Zhang, Selective catalytic reduction of NO with NH_3 at low temperatures over iron and manganese oxides on mesoporous silica, Appl. Catal. B 78 (2008) 309–314.
[5] M. Kang, E.D. Park, J.M. Kim, J.E. Yie, Manganese oxide catalysts for NO_x reduction with NH_3 at low temperature, Appl. Catal. A 327 (2007) 261–269.
[6] J.A. Sallivan, J.A. Doherty, NH_3 and urea in the selective catalytic reduction of NO_x over oxide-supported copper catalysts, Appl. Catal. B 55 (2005) 185–194.
[7] J.N. Armor, Catalytic reduction of nitrogen oxides with methane in the presence of excess oxygen, Catal. Today 26 (1995) 147–158.
[8] T. Tabata, M. Kokitsu, H. Ohtsuka, O. Okada, L.M.F. Sabatino, G. Bellussi, Study on catalysts of selective reduction of NO_x using hydrocarbons for natural gas engine, Catal. Today 27 (1996) 91–98.
[9] R. Zhang, A. Villanueva, H. Alamari, S. Kaliaguine, SCR of NO by propene over nanoscale $LaMn_{1-x}Cu_xO_3$ perovskites, Appl. Catal. A 307 (2006) 85–97.
[10] R. Zhang, A. Villanueva, H. Alamari, S. Kaliaguine, Optimization of mixed Ag catalysts for catalytic conversions of NO and C_3H_6, J. Catal. 237 (2006) 368–380.
[11] V.C. Belessi, T.V. Bakas, C.N. Costa, A.M. Efstathian, P.J. Pomonis, Synergistic effects of crystal phases and mixed valences in La–Sr–Ce–Fe–O mixed oxidic/perovskitic solids on their catalytic activity for the NO + CO reaction, Appl. Catal. B 28 (2000) 13–28.
[12] M.W. Chien, I.M. Pearson, K. Nobe, Reduction and adsorption kinetics of nitric oxide on cobalt perovskite catalysts, Ind. Eng. Chem. Res. 14 (1975) 131–134.
[13] A. Lindsteld Strömberg, M. Abul Milh, High-temperature catalytic reduction of nitrogen monoxide by carbon monoxide and hydrogen over $La_{1-x}Sr_xMO_3$ perovskites (M = Fe, Co) during reducing and oxidising conditions, Appl. Catal. A 116 (1994) 109–126.

[14] N. Mizuno, M. Tanaka, M. Misono, Reaction between carbon monoxide and nitrogen monoxide over perovskite-type mixed oxides, J. Chem. Soc., Faraday Trans. 88 (1992) 91–95.
[15] N. Mizuno, M. Yamato, M. Tanaka, M. Misono, Reactions of CO and NO over $La_{2-x}A'_xCu_{1-y}B'_yO_4$. A K_2NiF_4-type mixed oxide, Chem. Mater. 1 (1989) 232–236.
[16] L. Simonot, F. Garin, G. Maire, A comparative study of $LaCoO_3$, Co_3O_4 and a mix of $LaCoO_3$–Co_3O_4. II. Catalytic properties for the CO + NO reaction, Appl. Catal. B 11 (1997) 181–191.
[17] N.C. Costa, A.M. Efstathiou, Low temperature H_2-SCR of NO on a novel Pt/MgO–CeO_2 catalyst, Appl. Catal. B 72 (2007) 240–252.
[18] C.N. Costa, P.G. Savva, C. Andronikou, P.S. Lambrou, K. Polychronopoulou, V.C. Belessi, V.N. Stathopoulos, P.J. Pomonis, A.M. Efstathiou, An investigation of the NO/H_2/O_2 (lean de-NO_x) reaction on a highly active and selective Pt/$La_{0.7}Sr_{0.2}Ce_{0.1}FeO_3$ catalyst at low temperatures, J. Catal. 209 (2002) 456–471.
[19] N.C. Costa, V.N. Stathopoulos, V.C. Belessi, A.M. Efstathiou, An Investigation of the NO/H_2/O_2 (lean de-NO_x) reaction on a highly active and selective Pt/$La_{0.5}Ce_{0.5}MnO_3$ catalyst, J. Catal. 197 (2001) 350–364.
[20] D. Ferri, L. Forni, M.A.P. Dekkers, B.E. Nieuwenhuys, NO reduction by H_2 over perovskite-like mixed oxides, Appl. Catal. B 16 (1998) 339–345.
[21] A. Ueda, T. Nakao, M. Azuma, T. Kobayashi, Two conversion maxima at 373 and 573 K in the reduction of nitrogen monoxide with hydrogen over Pd/TiO_2 catalyst, Catal. Today 45 (1998) 135–138.
[22] M. Engelmann-Pirez, P. Granger, G. Leclercq, Investigation of the catalytic performances of supported noble metal based catalysis in the NO + H_2 reaction under lean conditions, Catal. Today 107 (2005) 315–322.
[23] C. Dujardin, I. Twagirashema, P. Granger, An operando spectroscopic investigation of the NO/H_2 reaction on $LaCoO_3$ and Pd-modified $LaCoO_3$. Influence of O_2 on catalyst performances and structure of adsorbed species, J. Phys. Chem. C 112 (2008) 17183–17192.
[24] F. Dhainaut, S. Pietrzyk, P. Granger, Kinetics of the NO/H_2 reaction on Pt/$LaCoO_3$: a combined theoretical and experimental study, J. Catal. 258 (2008) 296–305.
[25] F. Dhainaut, S. Pietrzyk, P. Granger, Kinetics of the NO + H_2 reaction over supported noble metal based catalysts: support effect on their adsorption properties, Appl. Catal. B 70 (2007) 100–110.
[26] Top Expert Project (2006–2009).
[27] A. Civera, M. Pavese, G. Saracco, V. Specchia, Combustion synthesis of perovskite-type catalysts for natural gas combustion, Catal. Today 83 (2003) 199–211.
[28] Z. Liu, P.J. Millington, J.E. Bailie, R.R. Rajaram, J.A. Anderson, A comparative study of the role of the support on the behaviour of iron based ammonia SCR catalysts, Micropor. Mesopor. Mater. 104 (2007) 159–170.
[29] R.J.K. Voorhoeve, J.P. Remeika, L.E. Trimble, A.S. Cooper, F.J. Disalvo, P.K. Gallagher, Perovskite-like $La_{1-x}K_xMnO_3$ and related compounds: solid state chemistry and the catalysis of the reduction of NO by CO and H_2, J. Solid State Chem. 14 (1975) 395–406.
[30] F. Dhainaut, S. Pietrzyk, P. Granger, NO + H_2 reaction on Pd/Al_2O_3 under lean conditions: kinetic study, Topics Catal. 42–43 (2007) 135–141.
[31] E. Cauda, D. Fino, G. Saracco, V. Specchia, Preparation and regeneration of a catalytic diesel particulate filter, Topics Catal. 30–31 (2004) 299–303.